

Basic Research

Percutaneous CO₂ Treatment Accelerates Bone Generation During Distraction Osteogenesis in Rabbits

Yohei Kumabe MD, Tomoaki Fukui MD, Shunsuke Takahara MD, Yu Kuroiwa MD, Michio Arakura MD, Keisuke Oe MD, Takahiro Oda MD, Kenichi Sawauchi MD, Takehiko Matsushita MD, Tomoyuki Matsumoto MD, Shinya Hayashi MD, Ryosuke Kuroda MD, Takahiro Niikura MD

Received: 11 September 2019 / Accepted: 14 April 2020 / Published online: 21 May 2020
Copyright © 2020 by the Association of Bone and Joint Surgeons

Abstract

Background Distraction osteogenesis has been broadly used to treat various structural bone deformities and defects. However, prolonged healing time remains a major problem. Various approaches including the use of low-intensity pulsed ultrasound, parathyroid hormone, and bone morphogenetic proteins (BMPs) have been studied to shorten the treatment period with limited success. Our previous studies of rats have reported that the transcutaneous application of CO₂ accelerates fracture repair and bone-defect healing in rats by promoting angiogenesis, blood flow, and endochondral ossification. This therapy may also accelerate bone generation during distraction

osteogenesis, but, to our knowledge, no study investigating CO₂ therapy on distraction osteogenesis has been reported. **Questions/purposes** We aimed to investigate the effect of transcutaneous CO₂ during distraction osteogenesis in rabbits, which are the most suitable animal as a distraction osteogenesis model for a lengthener in terms of limb size. We asked: Does transcutaneous CO₂ during distraction osteogenesis alter (1) radiographic bone density in the distraction gap during healing; (2) callus parameters, including callus bone mineral content, volumetric bone mineral density, and bone volume fraction; (3) the newly formed bone area, cartilage area, and angiogenesis, as well as the expression of interleukin-6 (IL-6), BMP-2, BMP-7, hypoxia-inducible factor (HIF) -1 α , and vascular endothelial growth factor (VEGF); and (4) three-point bend biomechanical strength, stiffness, and energy?

Methods Forty 24-week-old female New Zealand white rabbits were used according to a research protocol approved by our institutional ethical committee. A distraction osteogenesis rabbit tibia model was created as previously described. Briefly, an external lengthener was applied to the right tibia, and a transverse osteotomy was performed at the mid-shaft. The osteotomy stumps were connected by adjusting the fixator to make no gap. After a 7-day latency phase, distraction was continued at 1 mm per day for 10 days. Beginning the day after the osteotomy, a 20-minute transcutaneous application of CO₂ on the operated leg using a CO₂ absorption-enhancing hydrogel was performed five times per week in the CO₂ group (n = 20). Sham treatment with air was administered in the control group (n = 20). Animals were euthanized immediately after the distraction period (n = 10), 2 weeks (n = 10), and 4 weeks (n = 20) after completion of distraction. We

The institution of one or more of the authors (TN) has received, during the study period, funding from the Nakatomi Foundation, the ZENKYOREN (National Mutual Insurance Federation of Agricultural Cooperatives), and a Grant-in-Aid for Scientific Research (C) (JSPS KAKENHI Grant Number 17K10968). Each author certifies that his or her institution approved the animal protocol for this investigation and that all investigations were conducted in conformity with ethical principles of research.

Y. Kumabe, T. Fukui, S. Takahara, Y. Kuroiwa, M. Arakura, K. Oe, T. Oda, K. Sawauchi, T. Matsushita, T. Matsumoto, S. Hayashi, R. Kuroda, T. Niikura, Department of Orthopaedic Surgery, Kobe University Graduate School of Medicine, Kobe, Japan

T. Niikura (✉), Department of Orthopaedic Surgery, Kobe University Graduate School of Medicine, 7-5-1 Kusunoki-cho, Chuo-ku, Kobe 650-0017, Japan, Email: tniikura@med.kobe-u.ac.jp

All ICMJE Conflict of Interest Forms for authors and *Clinical Orthopaedics and Related Research*® editors and board members are on file with the publication and can be viewed on request.

performed bone density quantification on the plain radiographs to evaluate consolidation in the distraction gap with image analyzing software. Callus parameters were measured with micro-CT to assess callus microstructure. The newly formed bone area and cartilage area were measured histologically with safranin O/fast green staining to assess the progress of ossification. We also performed immunohistochemical staining of endothelial cells with fluorescein-labeled isolectin B4 and examined capillary density to evaluate angiogenesis. Gene expressions in newly generated callus were analyzed by real-time polymerase chain reaction. Biomechanical strength, stiffness, and energy were determined from a three-point bend test to assess the mechanical strength of the callus.

Results Radiographs showed higher pixel values in the distracted area in the CO₂ group than the control group at Week 4 of the consolidation phase (0.98 ± 0.11 [95% confidence interval 0.89 to 1.06] versus 1.19 ± 0.23 [95% CI 1.05 to 1.34]; $p = 0.013$). Micro-CT demonstrated that bone volume fraction in the CO₂ group was higher than that in the control group at Week 4 ($5.56 \pm 3.21\%$ [95% CI 4.32 to 6.12%] versus $11.90 \pm 3.33\%$ [95% CI 9.63 to 14.25%]; $p = 0.035$). There were no differences in any other parameters (that is, callus bone mineral content at Weeks 2 and 4; volumetric bone mineral density at Weeks 2 and 4; bone volume fraction at Week 2). At Week 2, rabbits in the CO₂ group had a larger cartilage area compared with those in the control group ($2.09 \pm 1.34\text{ mm}^2$ [95% CI 1.26 to 2.92 mm²] versus $5.10 \pm 3.91\text{ mm}^2$ [95% CI 2.68 to 7.52 mm²]; $p = 0.011$). More newly formed bone was observed in the CO₂ group than the control group at Week 4 ($68.31 \pm 16.32\text{ mm}^2$ [95% CI 58.19 to 78.44 mm²] versus $96.26 \pm 19.37\text{ mm}^2$ [95% CI 84.25 to 108.26 mm²]; $p < 0.001$). There were no differences in any other parameters (cartilage area at Weeks 0 and 4; newly formed bone area at Weeks 0 and 2). Immunohistochemical isolectin B4 staining showed greater capillary densities in rabbits in the CO₂ group than the control group in the distraction area at Week 0 and surrounding tissue at Weeks 0 and 2 (distraction area at Week 0, $286.54 \pm 61.55/\text{mm}^2$ [95% CI 232.58 to 340.49] versus $410.24 \pm 55.29/\text{mm}^2$ [95% CI 361.78 to 458.71]; $p < 0.001$; surrounding tissue at Week 0 $395.09 \pm 68.16/\text{mm}^2$ [95% CI 335.34 to 454.83] versus $589.75 \pm 174.42/\text{mm}^2$ [95% CI 436.86 to 742.64]; $p = 0.003$; at Week 2 $271.22 \pm 169.42/\text{mm}^2$ [95% CI 122.71 to 419.73] versus $508.46 \pm 49.06/\text{mm}^2$ [95% CI 465.45 to 551.47]; $p < 0.001$ respectively). There was no difference in the distraction area at Week 2. The expressions of BMP-2 at Week 2, HIF1- α at Week 2 and VEGF at Week 0 and 2 were greater in the CO₂ group than in the control group (BMP-2 at Week 2 3.84 ± 0.83 fold [95% CI 3.11 to 4.58] versus 7.32 ± 1.63 fold [95% CI 5.88 to 8.75]; $p < 0.001$; HIF1- α at Week 2, 10.49 ± 2.93 fold [95% CI 7.91 to 13.06] versus 20.74 ± 11.01 fold [95% CI

11.09 to 30.40]; $p < 0.001$; VEGF at Week 4 4.80 ± 1.56 fold [95% CI 3.43 to 6.18] versus 11.36 ± 4.82 fold [95% CI 7.13 to 15.59]; $p < 0.001$; at Week 2 31.52 ± 8.26 fold [95% CI 24.27 to 38.76] versus 51.05 ± 15.52 fold [95% CI 37.44 to 64.66]; $p = 0.034$, respectively). There were no differences in any other parameters (BMP-2 at Week 0 and 4; BMP-7 at Weeks 0, 2 and 4; HIF-1 α at Weeks 0 and 4; IL-6 at Weeks 0, 2 and 4; VEGF at Week 4). In the biomechanical assessment, ultimate stress and failure energy were greater in the CO₂ group than in the control group at Week 4 (ultimate stress $259.96 \pm 74.33\text{ N}$ [95% CI 167.66 to 352.25] versus $422.45 \pm 99.32\text{ N}$ [95% CI 299.13 to 545.77]; $p < 0.001$, failure energy $311.32 \pm 99.01\text{ Nmm}$ [95% CI 188.37 to 434.25] versus $954.97 \pm 484.39\text{ Nmm}$ [95% CI 353.51 to 1556.42]; $p = 0.003$, respectively). There was no difference in stiffness ($216.77 \pm 143.39\text{ N/mm}$ [95% CI 38.73 to 394.81] versus $223.68 \pm 122.17\text{ N/mm}$ [95% CI 71.99 to 375.37]; $p = 0.92$).

Conclusion Transcutaneous application of CO₂ accelerated bone generation in a distraction osteogenesis model of rabbit tibias. As demonstrated in previous studies, CO₂ treatment might affect bone regeneration in distraction osteogenesis by promoting angiogenesis, blood flow, and endochondral ossification.

Clinical Relevance The use of the transcutaneous application of CO₂ may open new possibilities for shortening healing time in patients with distraction osteogenesis. However, a deeper insight into the mechanism of CO₂ in the local tissue is required before it can be used in future clinical practice.

Introduction

Distraction osteogenesis is a well-established surgical technique in pediatric and adult orthopaedics to treat various pathologic conditions such as bone deformities, large bone defects after trauma, leg-length discrepancy, and bone resection for malignant bone tumors and osteomyelitis [32, 43, 44, 48]. Typically, when performing distraction osteogenesis, a transverse bone section is created, and gradual distraction of the two bone fragments is initiated. There is newly generated bone tissue in the gap between the bone fragments. Three temporal phases exist in distraction osteogenesis: a latency phase, a distraction phase, and a consolidation phase [8, 20, 21]. A limitation of this approach is the long duration required for the maturation, mineralization, and consolidation of newly formed bone tissue. The external device must be kept at the site throughout this prolonged healing time, which can lead to social, psychological, and physical burdens [10, 48]. To shorten the treatment period, various materials, including mesenchymal stem cells, fibroblast growth factor, bone morphogenetic proteins (BMPs), prostaglandin E receptor agonists, and

bone conduction agents such as calcium sulfate have been used. However, these materials have problems regarding cost, accessibility, effectiveness, and duration of effect [4, 28, 29, 34, 46, 54, 61, 62]. Therefore, new techniques are of interest to improve distraction osteogenesis.

Our research group designed a system for the topical, cutaneous application of CO₂ using a novel hydrogel, which can facilitate CO₂ absorption through the skin into the deep area within a limb [45, 53]. Studies using a rat femoral fracture model [30] and rat femoral defect model [33] by our group found that CO₂ treatment increased the expression of vascular endothelial growth factor (VEGF) and blood flow at the fracture and bone defect sites, resulting in accelerated endochondral ossification, fracture repair, and bone defect healing. It has been advocated that angiogenesis and blood flow are essential components for bone generation in distraction osteogenesis and in fracture healing [1, 9], and therefore, this therapy may also be effective in distraction osteogenesis. To our knowledge, there are no reported studies investigating CO₂ therapy on distraction osteogenesis, and hence we theorized that the cutaneous application of CO₂ could also be effective in accelerating bone generation in distraction osteogenesis in the current study. We adopted a rabbit model of distraction osteogenesis, which is easier to operate on than a rat model in terms of limb size and has been widely used for other distraction osteogenesis studies [27, 31, 34-36, 40, 42, 46, 51, 54].

We asked: Does transcutaneous CO₂ during distraction osteogenesis alter (1) radiographic bone density in the distraction gap during healing; (2) callus parameters, including callus bone mineral content, volumetric bone mineral density, and bone volume fraction; (3) the newly formed bone area, cartilage area, and angiogenesis, as well as the expression of interleukin-6 (IL-6), BMP-2, BMP-7, hypoxia-inducible factor (HIF) -1 α , and VEGF; and (4) three-point bend biomechanical strength, stiffness, and energy?

Materials and Methods

Animal Model

Forty seven 24-week old female New Zealand white rabbits (Japan SLC Inc, Hamamatsu, Japan) weighing 3.2 kg to 3.9 kg were used in this study. Seven were excluded because of fracture or infection within 2 weeks after surgery; 40 rabbits were finally included. Rabbits were randomized into treatment and sham treatment groups. According to our preliminary experiment, a power analysis was performed using an estimated 0.22 difference in pixel values on a plain radiograph at week 4 between two groups. With beta = 0.80 and alpha = 0.05, we determined that 10 rabbits were adequate in each group. The rabbits were anesthetized with inhalational anesthesia with 3% to 5% isoflurane (Fujifilm

Wako Pure Chemical Corp, Osaka, Japan) per 1.5 to 4.0 L/min of 100% O₂ using a mask, intravenous injection of 30 mg/kg of pentobarbital sodium (Kyoritsu Seiyaku Corp, Tokyo, Japan), and local injection of 30 mg/kg of lidocaine hydrochloride (Aspen Japan Co Ltd., Tokyo, Japan). The distraction osteogenesis model was created based on Maruno's method [40]. Hair was shaved, and a longitudinal skin incision was made on the medial aspect of the right tibia, and the periosteum was carefully stripped along with the surrounding soft tissue and fascia. Four half-pins, 2.0-mm in diameter, were inserted with a distance of 20 mm between the two pairs of pins, and an external fixator (OrthofixM-100, Verona, Italy) was applied to connect the four pins. A transverse osteotomy using an oscillating saw was performed at a site 10 mm distal to the tibiofibular junction. During osteotomy, saline was dripped onto the osteotomy site to prevent heating. The osteotomy stumps were connected by adjusting the fixator to make no gap. The hind legs were loaded immediately after surgery, without movement restriction. After a waiting period of 7 days, distraction was performed at a rate of 1 mm/day by adjusting the fixator once daily for 10 days (total: 10 mm, approximately 10% of the original bone length). Animals were euthanized with an overdose of pentobarbital sodium (150 mg/kg) at 0, 2, and 4 weeks after the consolidation phase after distraction was completed. After removing the external fixator device for assessment, we obtained the rabbits' tibiae (Fig. 1). All rabbits were housed separately in standard cages with temperature control (20° C to 23° C) and had free access to food and water. All protocols of this research study were approved by the Animal Ethics Committee of Kobe University.

CO₂ Treatment

The animals were divided into two groups: the CO₂ and control groups (n = 20 rabbits in each group). In both groups, the rabbits were put in an animal holder, and hydrogel was applied. The hydrogel had a pH of 5.5 and consisted of carbomer, glycerin, sodium hydroxide, sodium alginate, sodium dihydrogen phosphate, methylparaben, and de-ionized water. The limb was covered with a polyethylene bag filled with either 100% CO₂ (treatment group) or air (control group) for 20 minutes. In the CO₂ group, the air was removed from the bag before CO₂ gas filling and gas was added intermittently during treatment to keep the level of CO₂ in the bag. This treatment was performed five times per week after the operation until the animals were euthanized.

Radiographic Analysis

To evaluate radiographic bone density, we performed plain radiography at Weeks 0, 1, 2, 3, and 4 of the consolidation

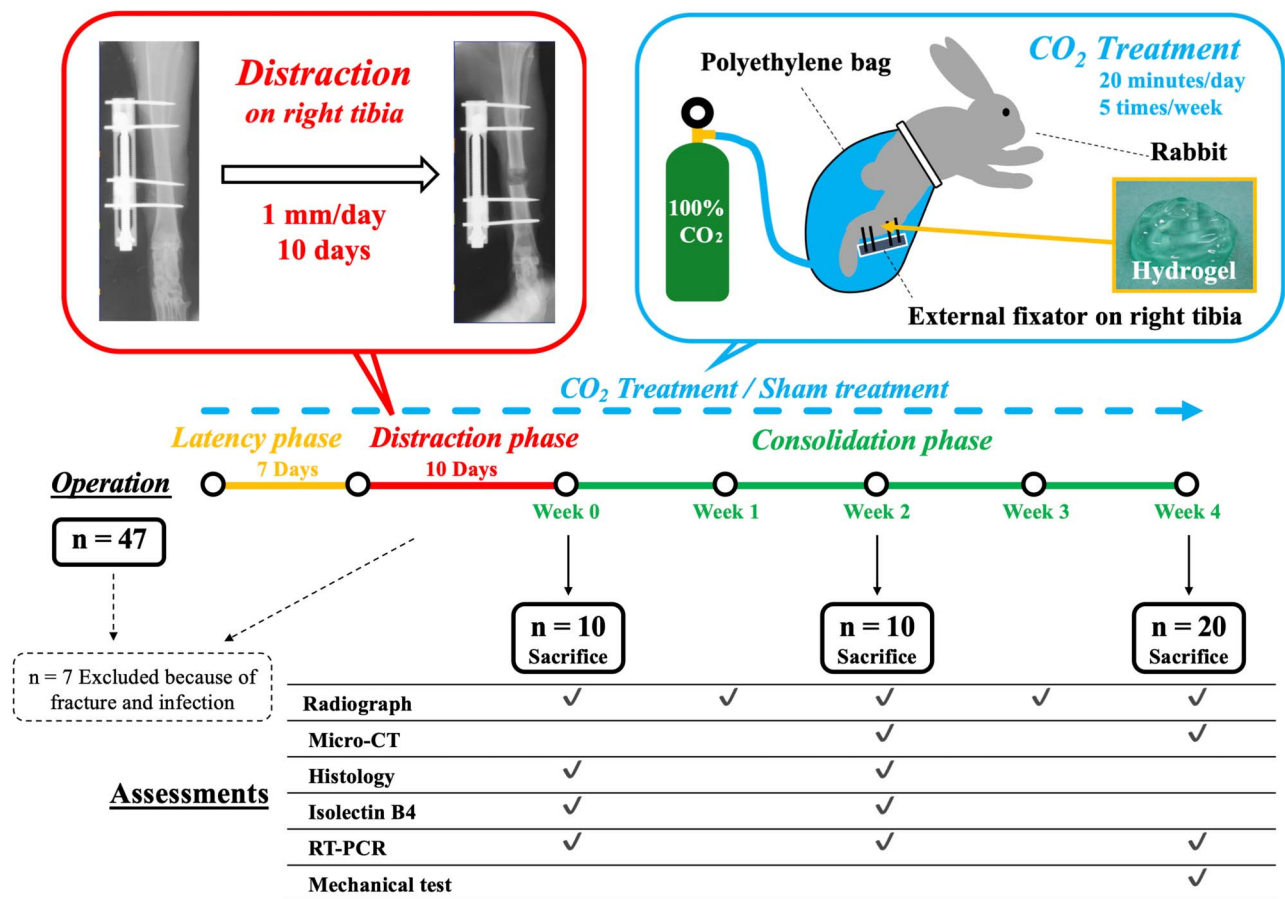


Fig. 1 This schema shows the study design and the number of animals involved at each stage; RT-PCR = real-time polymerase chain reaction.

phases. With the rabbits under inhalational anesthesia with isoflurane, AP radiographs of the lengthened limb were taken with a VPX30E system (Canon Medical Systems, Tochigi, Japan). Using sequential plain radiographs, we compared the bone gap and bone density of rabbits in the CO₂ group with those of rabbits in the control group. We calculated pixel values of the distraction gap in the Image J program (National Institutes of Health, Bethesda, MD, USA) using plain radiographs and normalized these values by the pixel values of the ipsilateral tibial shaft. Bone density was quantified by analyzing pixels using Kim et al.'s method [27]. After the pixel values were normalized, the bone density of the distraction gap could be quantitatively compared between the two groups.

Micro-CT Measurement

To quantify callus formation, we performed micro-CT on the harvested, lengthened tibiae of five animals in each group at Weeks 2 and 4 of the consolidation phase using a micro-CT Imager (R_mCT2 FX, Rigaku Corp, Tokyo,

Japan). After scanning, we made a three-dimensional reconstruction using built-in software. The region of interest was set as a distracted area of 10 mm and also extended 5-mm proximally and distally, resulting in a region of interest of 20 mm. The following parameters of the callus were calculated from the region of interest using bone microstructure software (TRI/3D-BON-FCS64, Ratoc System Engineering, Tokyo, Japan): tissue mineral density, callus bone mineral content, volumetric bone mineral density, and bone volume fraction. Callus bone mineral content was calibrated by scanning hydroxyapatite phantoms of known densities that were provided by the system manufacturer.

Nondecalcified Frozen Histology and Immunohistochemical Staining

We assessed newly formed bone area and cartilage area with non-decalcified frozen histology, and we assessed angiogenesis with immunohistochemical staining. We used Kawamoto's [25] method to prepare frozen sections of nondecalcified tibiae. Briefly, at 0, 2, and 4 weeks of the

consolidation phase, specimens were immersed in cooled embedding medium (Super Cryoembedding Medium L-1; Section-Lab, Hiroshima, Japan) and quickly frozen in liquid nitrogen to form a frozen block. Sagittal sections (5- μ m thick) were mounted on adhesive film (Cryofilm, Section-Lab Co. Ltd, Hiroshima, Japan) with a cryostat (Leica, Nussloch, Germany) and stained with safranin-O fast green for histologic assessment. The newly formed bone and cartilage areas were captured with a microscope (BZ-710; Keyence Corp, Osaka, Japan) and measured with the Image J program (National Institutes of Health, Bethesda, MD, USA). Additionally, at 0 and 2 weeks of the consolidation phase, immunohistochemical staining of endothelial cells was performed with fluorescein-labeled isolectin B4 (Vector Laboratories, Burlingame, CA, USA) to evaluate angiogenesis in five animals of each group [15]. Nuclear staining was performed with a 49,6-diamidino-2-phenylindole solution. The capillary density was examined under a microscope; the numbers of capillaries in five randomly selected fields in the distracted area and surrounding tissue were counted using built-in software, and the mean and SD were calculated.

Assessment of Gene Expression

Gene expression of IL-6, BMP-2, BMP-7, HIF-1 α and VEGF were measured at 0, 2, and 4 weeks of the consolidation phase in five animals in each group using real-time polymerase chain reaction. We assessed these genes because IL-6 inhibits the differentiation of mesenchymal cells into mature osteoblastic lineage cells, suggesting that it is one of the key mechanisms in distraction osteogenesis [1]; BMP-2 and BMP-7 are multifunctional growth factors implicated in bone formation [58]; a previous study showed that strong expression of HIF-1 α , which activates angiogenic factor expression, thus increasing oxygen supply, is observed in distraction gap [3]; and, evidence suggests that VEGF is essential for both the formation of new blood vessels and new bone formation through skeletal cell differentiation [22]. Newly generated callus tissue was harvested from the distracted area. Total RNA was extracted from tissue using an RNeasy Mini Kit (Qiagen, Valencia, CA, USA) and reverse-transcribed into single-stranded DNA using a high-capacity cDNA reverse transcription kit (Applied Biosystems, Foster City, CA, USA). The real-time polymerase chain reaction was performed in triplicate on the cDNA with an ABI PRISM 7700 Sequence Detection System and SYBR Green reagent (Applied Biosystems, Foster City, CA, USA). The expression level of each gene was first normalized with respect to glyceraldehyde-3-phosphate dehydrogenase, which is a well-known housekeeping gene serving as an internal control. All results are presented as the fold-change relative

to the control group at Week 0, which was normalized to a value of 1 ($\Delta\Delta$ Ct method) [37].

Biomechanical Assessment

The mechanical properties (ultimate stress, failure energy, and stiffness) of the newly formed bone tissue was assessed via three-point bending of the harvested whole bone at 4 weeks of the consolidation phase in five rabbits in each group. The three-point bend test of the lengthened tibia was performed with a materials testing machine (MZ-500S; Maruto Instrument Company, Tokyo, Japan). Specimens were kept at room temperature and moist throughout testing with saline to prevent dehydration. All supports and loading noses had a radius of 1.5 mm, and the span length of the two supports was 20 mm. Each bone was positioned with the posterior surface downward, and the upper support applied force directly to the middle point of the healing callus. The testing conditions provided no preload and were displacement-controlled at a constant velocity of the upper support of 2 mm per minute. During the three-point bend test, load and displacement were recorded and analyzed using an attached PC and software supplied with the materials testing machine. The ultimate stress (in N), failure energy (in Nmm) and extrinsic stiffness (in N/mm) were determined from the load-deformation curve.

Statistical Analysis

All quantitative data are presented as the mean \pm SD. Comparison of pixel values calculated from radiographic density, callus parameters in micro-CT, the newly formed bone area, cartilage area, and the numbers of capillaries in histological assessment, fold changes in gene expression assessment, and the mechanical properties assessed via three-point bend test between the two groups were performed with the Brunner-Munzel test using BellCurve for Excel (Social Survey Research Information Co Ltd, Tokyo, Japan). A p value of less than 0.05 was set as statistically significant. A post-hoc power analysis was performed for each measurement using G*Power 3.1.9.2 (Franz Paul) software.

Results

Radiographic Bone Density Quantification in the Distraction Gap

Representative sequential weekly plain radiographs (Fig. 2A) and representative radiographs at Week 3 (Fig. 2B) of both groups are shown. Radiographs showed higher pixel values in the distracted area in the CO₂ group

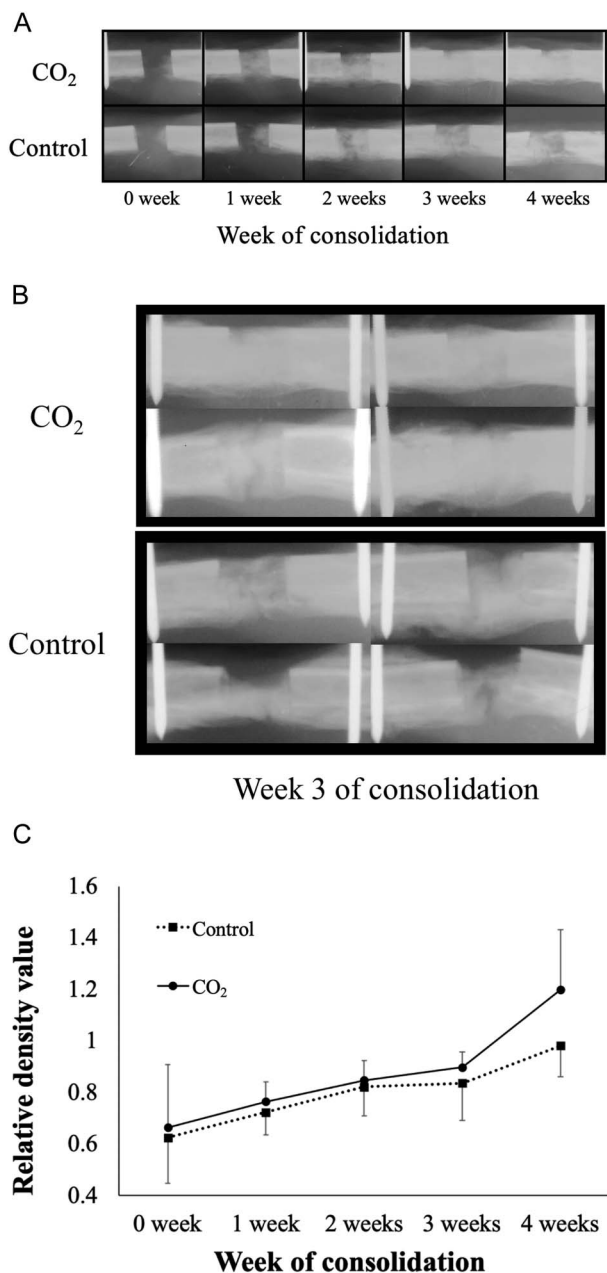


Fig. 2 A-C (A) Sequential plain radiographs of the distracted area. (B) Plain radiographs of the distracted area at Week 3. (C) Radiographs of the CO₂ group showed higher pixel values (relative density) than did those in the control group at week 4 of the consolidation phase (data shown are mean and SD).

than the control group at Week 4 of the consolidation phase (0.98 ± 0.11 [95% confidence interval 0.89 to 1.06] versus 1.19 ± 0.23 [95% CI 1.05 to 1.34]; p = 0.013). There were no differences before Week 4 (at Week 0 0.62 ± 0.17 [95% CI 0.54 to 0.70] versus 0.66 ± 0.24 [95% CI 0.55 to 0.77]; p = 0.82, at Week 1 0.72 ± 0.08 [95% CI 0.67 to 0.77] versus 0.76 ± 0.07 [95% CI 0.72 to 0.80]; p = 0.21, at

Week 2 0.82 ± 0.11 [95% CI 0.76 to 0.88] versus 0.84 ± 0.07 [95% CI 0.80 to 0.88]; p = 0.57, at Week 3 0.83 ± 0.14 [95% CI 0.74 to 0.92] versus 0.89 ± 0.06 [95% CI 0.86 to 0.93]; p = 0.33, respectively) (Fig. 2C).

Callus Parameters Measured with Micro-CT

Micro-CT demonstrated that bone volume fraction (bone volume/total callus volume) in the CO₂ group was higher than that in the control group at Week 4 (5.56 ± 3.21 % [95% CI 4.32 to 6.12 %] versus 11.90 ± 3.33 % [95% CI 9.63 to 14.25]; p = 0.035). There were no differences in any other parameters (callus bone mineral content at Week 2 99.07 ± 29.37 mg [95% CI 63.93 to 120.28] versus 244.05 ± 28.09 mg [95% CI 171.80 to 307.95]; p = 0.052, at Week 4 124.74 ± 99.12 mg [95% CI 94.37 to 136.18] versus 331.69 ± 97.94 mg [95% CI 262.63 to 398.27]; p = 0.064, volumetric bone mineral density at Week 2 414.92 ± 31.00 mg/cm³ [95% CI 380.95 to 428.49] versus 540.80 ± 21.02 mg/cm³ [95% CI 498.87 to 582.23]; p = 0.14, at Week 4 441.60 ± 60.14 mg/cm³ [95% CI 417.93 to 452.21] versus 548.82 ± 35.81 mg/cm³ [95% CI 521.56 to 567.54]; p = 0.56, bone volume fraction at Week 2 4.66 ± 1.20% [95% CI 3.23 to 5.66] versus 8.74 ± 1.06% [95% CI 6.43 to 10.72]; p = 0.22, respectively) (Table 1).

Newly Formed Bone Area and Cartilage Area in Non-decalcified Frozen Histology and the Numbers of Capillaries in Immunohistochemical Imaging

Only a small amount of cartilage and newly formed bone were observed in rabbits in both groups at Week 0 of consolidation period (0.75 ± 1.37 mm² [95% CI -0.10 to 1.60] versus 1.19 ± 1.72 mm² [95% CI 0.12 to 2.26]; p = 0.098). At Week 2, rabbits in the CO₂ group had a larger cartilage area than those in the control group (2.09 ± 1.34 mm² [95% CI 1.26 to 2.92] versus 5.10 ± 3.91 mm² [95% CI 2.68 to 7.52]; p = 0.011). The cartilage area decreased in rabbits in the CO₂ group at Week 4 compared with Week 2; in contrast, thick cartilage tissue remained in rabbits in the control group at Week 4 (5.16 ± 4.48 mm² [95% CI 2.38 to 7.94] versus 3.67 ± 3.14 mm² [95% CI 1.72 to 5.62]; p = 0.41). Moreover, rabbits in the CO₂ group exhibited greater newly formed bone than those in the control group did at Week 4, indicating accelerated endochondral ossification in the CO₂ group (68.31 ± 16.32 mm² [95% CI 58.19 to 78.44] versus 96.26 ± 19.37 mm² [95% CI 84.25 to 108.26]; p < 0.001). There were no differences in newly formed bone area at Week 0 and 2 (22.18 ± 13.17 mm² [95% CI 14.01 to 30.34] versus 17.86 ± 10.23 mm² [95% CI 11.51 to 24.20]; p = 0.46, 57.77 ± 6.17 mm² [95% CI 53.94 to 61.60] versus

Table 1. Bone mineral content, bone mineral density and bone volume fraction at Weeks 2 and 4

	Week of consolidation	Group	Bone mineral content (mg)	95% confidence interval	p value	
Bone mineral content	Week 2	Control	99.07 ± 29.37	63.93 to 120.28	0.052	
		CO ₂	244.05 ± 28.09	171.80 to 307.95		
	Week 4	Control	124.74 ± 99.12	94.37 to 136.18	0.064	
		CO ₂	331.69 ± 97.94	262.63 to 398.27		
Bone mineral density	Week 2	Control	414.92 ± 31.00	380.95 to 428.49	0.14	
		CO ₂	540.80 ± 21.02	498.87 to 582.23		
	Week 4	Control	441.60 ± 60.14	417.93 to 452.21	0.56	
		CO ₂	548.82 ± 35.81	521.56 to 567.54		
	Bone volume fraction	Week 2	Control	4.66 ± 1.20	3.23 to 5.66	0.22
			CO ₂	8.74 ± 1.06	6.43 to 10.72	
Week 4		Control	5.56 ± 3.21	4.32 to 6.12	0.035	
		CO ₂	11.90 ± 3.33	9.63 to 14.25		

54.17 ± 12.38 mm² [95% CI 46.50 to 61.85]; p = 0.11, respectively) (Fig. 3A-B).

Immunohistochemical isolectin B4 staining in tissue samples showed greater capillary densities in rabbits in the CO₂ group than in those in the control group in the distraction area and surrounding tissue at Week 0 and in the surrounding tissue at Week 2 (distraction area at Week 0 286.54 ± 61.55 /mm² [95% CI 232.58 to 340.49] versus 410.24 ± 55.29/mm² [95% CI 361.78 to 458.71]; p < 0.001, surrounding tissue at Week 0 395.09 ± 68.16/mm² [95% CI 335.34 to 454.83] versus 589.75 ± 174.42/mm² [95% CI 436.86 to 742.64]; p = 0.003, at Week 2 271.22 ± 169.42/mm² [95% CI 122.71 to 419.73] versus 508.46 ± 49.06/mm² [95% CI 465.45 to 551.47]; p < 0.001 respectively) (Fig. 4). There was no difference in the distraction area at Week 2 (277.92 ± 136.56/mm² [95% CI 158.21 to 397.62] versus 351.97 ± 192.35/mm² [95% CI 183.37 to 520.57]; p = 0.52) (Table 2).

Gene Expression in Newly Generated Callus

Real-time polymerase chain reaction revealed that the expressions of BMP-2 at Week 2, HIF1-α at Week 2 and VEGF at Week 0 and 2 were greater in the CO₂ group than in the control group (BMP-2 at Week 2 3.84 ± 0.83 fold [95% CI 3.11 to 4.58 fold] versus 7.32 ± 1.63 fold [95% CI 5.88 to 8.75]; p < 0.001, HIF1-α at Week 2 10.49 ± 2.93 fold [95% CI 7.91 to 13.06] versus 20.74 ± 11.01 fold [95% CI 11.09 to 30.40]; p < 0.001, VEGF at Week 0 4.80 ± 1.56 fold [95% CI 3.43 to 6.18] versus 11.36 ± 4.82 fold [95% CI 7.13 to 15.59]; p < 0.001, at Week 2 31.52 ± 8.26 fold [95% CI

24.27 to 38.76] versus 51.05 ± 15.52 fold [95% CI 37.44 to 64.66]; p = 0.034, respectively). There were no differences in any other parameters (BMP-2 at Week 0 1.61 ± 1.51 fold [95% CI 0.28 to 2.93] versus 0.97 ± 0.71 fold [95% CI 0.35 to 1.60]; p = 0.63, at Week 4 5.52 ± 2.94 fold [95% CI 2.94 to 8.10] versus 5.06 ± 2.76 fold [95% CI 2.63 to 7.49]; p = 0.77, BMP-7 at Week 0 0.59 ± 0.30 fold [95% CI 0.32 to 0.85] versus 0.77 ± 0.63 fold [95% CI 0.21 to 1.33]; p = 0.78, at Week 2 4.28 ± 2.25 fold [95% CI 2.30 to 6.26] versus 3.93 ± 2.85 fold [95% CI 1.43 to 6.43]; p = 0.77, at Week 4 9.15 ± 6.36 fold [95% CI 3.57 to 14.73] versus 11.81 ± 7.03 fold [95% CI 5.64 to 17.98]; p = 0.63, HIF-1α at Week 0 1.24 ± 0.43 fold [95% CI 0.86 to 1.62] versus 1.21 ± 0.34 fold [95% CI 0.90 to 1.51]; p < 0.92, at Week 4 5.82 ± 1.74 fold [95% CI 4.29 to 7.35] versus 4.87 ± 0.68 fold [95% CI 4.27 to 5.48]; p = 0.47, IL-6 at Week 0 1.25 ± 0.41 fold [95% CI 0.89 to 1.62] versus 2.03 ± 1.12 fold [95% CI 1.05 to 3.02]; p = 0.27, at Week 2 2.92 ± 2.40 fold [95% CI 0.82 to 5.03] versus 1.84 ± 2.43 fold [95% CI -0.29 to 3.97]; p = 0.32, at Week 4 3.20 ± 3.62 fold [95% CI 0.03 to 6.38] versus 2.66 ± 1.60 fold [95% CI 1.25 to 4.07]; p = 0.93, VEGF at Week 4 7.97 × 10⁵ ± 10.92 fold [95% CI -2.72 × 10⁵ to 18.67 × 10⁵] versus 9.22 × 10⁵ ± 11.91 × 10⁵ fold [95% CI -1.22 × 10⁵ to 19.66 × 10⁵]; p = 0.92, respectively) (Fig. 5).

Three-point Bend Behavior

In the biomechanical assessment, three-point bend ultimate stress and failure energy were greater in the CO₂ group than in the control group at Week 4 (ultimate stress 259.96 ± 74.33 N [95% CI 167.66 to -352.25] versus 422.45 ±

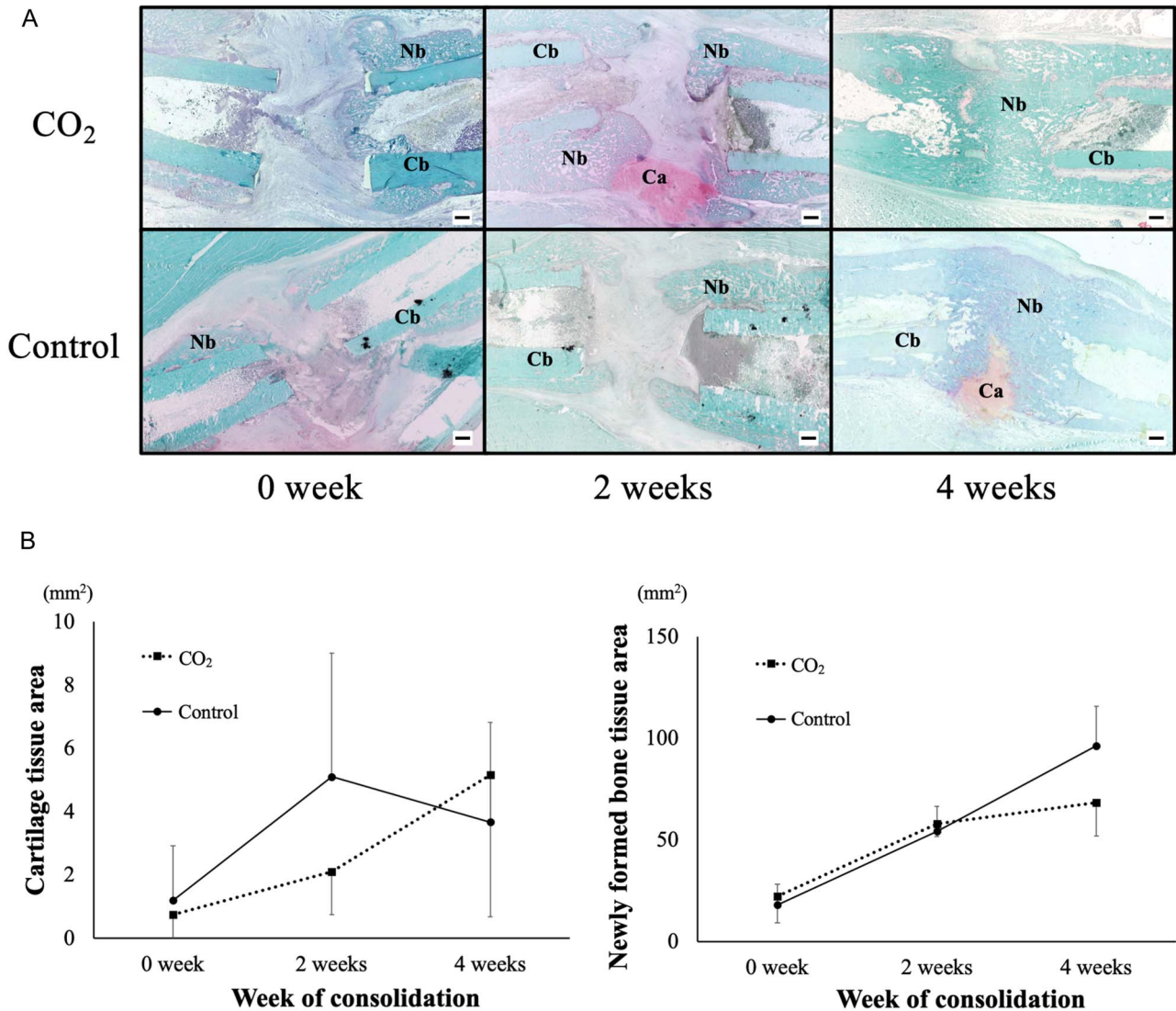


Fig 3 A-B (A) These are representative histologic sections at the distracted area stained with safranin-O/fast green. (B) The mean and SD for areas of the cartilage tissue and newly formed bone at distracted area at Weeks 0, 2, and 4 are shown. At Week 2, the cartilage area was larger in the CO₂ group than in the control group. The CO₂ group showed greater newly formed bone area (shown are mean and SD) than did the control group at Week 4. Ca = cartilage, Nb = newly formed bone, Cb = cortical bone, Bar = 1 mm.

99.32 N [95% CI 299.13 to 545.77]; $p < 0.001$, failure energy 311.32 ± 99.01 Nmm [95% CI 188.37 to 434.25] versus 954.97 ± 484.39 Nmm [95% CI 353.51 to 1556.42]; $p = 0.003$, respectively). There was no difference in stiffness (216.77 ± 143.39 N/mm [95% CI 38.73 to 394.81] versus 223.68 ± 122.17 N/mm [95% CI 71.99 to 375.37]; $p = 0.92$) (Fig. 6).

Discussion

CO₂ therapy has been reported to have a therapeutic effect in patients with certain cardiac diseases and skin disorders [19,

49]. The therapeutic effects of CO₂ may occur due to increased blood flow, microcirculation, and nitric oxide-dependent formation of new capillaries, as well as because of an increase in the partial pressure of oxygen in local tissue (the Bohr effect) [24]. We designed a system for the topical, cutaneous application of CO₂ using a novel hydrogel in which CO₂ readily dissolves [54]. This easy and non-invasive CO₂ treatment induces the artificial Bohr effect, in which blood flow is increased and oxygen is disassociated from hemoglobin in the soft tissues surrounding bone. This effect can be observed immediately after the CO₂ treatment starts. Our previous studies have reported that the transcutaneous application of CO₂ accelerates fracture repair and

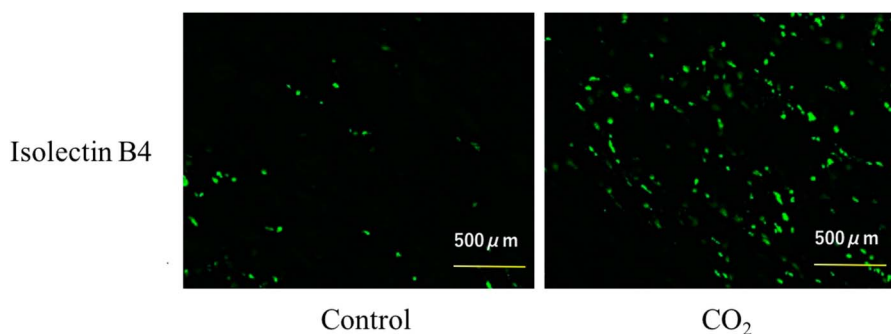


Fig. 4 These representative images show fluorescent vascular staining of isolectin B4 in the distracted area at Week 0. Capillaries appear in green.

bone-defect healing in rats by promoting angiogenesis, blood flow, and endochondral ossification [30, 33]. This therapy may also accelerate bone generation during distraction osteogenesis, but, to our knowledge, no study investigating CO₂ therapy on distraction osteogenesis has been reported. Therefore, we investigated the effect of transcutaneous CO₂ during distraction osteogenesis with a rabbit model. We found that radiographic density in the distraction gap and bone volume fraction in the distracted callus at 4 weeks of consolidation in the CO₂ group were greater than the control group. A larger cartilage area at Week 2 and greater newly formed bone at Week 4 were observed in the CO₂ group than the control group in the histology. Greater capillary densities were observed in the CO₂ group than the control group in the distraction area at Week 0 and surrounding tissue at Week 0, and 2. The expressions of BMP-2 at Week 2, HIF1-α at Week 2 and VEGF at Week 0 and 2 were greater in the CO₂ group than in the control group. Ultimate stress and failure energy of distracted callus were greater in the CO₂ group than in the control group at Week 4. Collectively, these results indicate that CO₂ treatment accelerates bone generation in a rabbit model of distraction osteogenesis.

The limitations of the present study are that we observed the animals until Week 4 of the consolidation phase, when ossification progressed from each side to the center of the distracted site, whereas, we did not observe the complete bone generation process, including remodeling and new medullary canal formation. To observe all stages of bone generation, a longer study period of more than 8 weeks would be needed [40, 51], and future studies should seek to provide this information. Also, we used only female rabbits. Generally, both male and female rabbits could be used for our distraction osteogenesis model, but we chose female rabbits because they are more docile and less likely to fight, thus minimizing the possibility of breaking their leg and the polyethylene bag during CO₂ treatment.

Plain radiographs revealed that the density of the distraction area was greater in the CO₂ group than the control group and micro-CT showed higher bone volume fraction of the callus in the CO₂ group than the control group at Week 4 of the consolidation phase. These findings indicated that maturing from callus to bone at the distracted area has been accelerated by CO₂ therapy at Week 4 of the consolidation phase.

Table 2. Capillary density in the distracted and surrounding areas at Weeks 0 and 2

	Week of consolidation	Group	Capillary density (/mm ²)	95% confidence interval	p value
Capillary density in the distracted area	Week 0	Control	286.54 ± 61.55	232.58 to 340.49	< 0.001
		CO ₂	410.24 ± 55.29	361.78 to 458.71	
	Week 2	Control	277.92 ± 136.56	158.21 to 397.62	0.52
		CO ₂	351.97 ± 192.35	183.37 to 520.57	
Capillary density in the surrounding area	Week 0	Control	395.09 ± 68.16	335.34 to 454.83	0.003
		CO ₂	589.75 ± 174.42	436.86 to 742.64	
	Week 2	Control	271.22 ± 169.42	122.71 to 419.73	< 0.001
		CO ₂	508.46 ± 49.06	465.45 to 551.47	

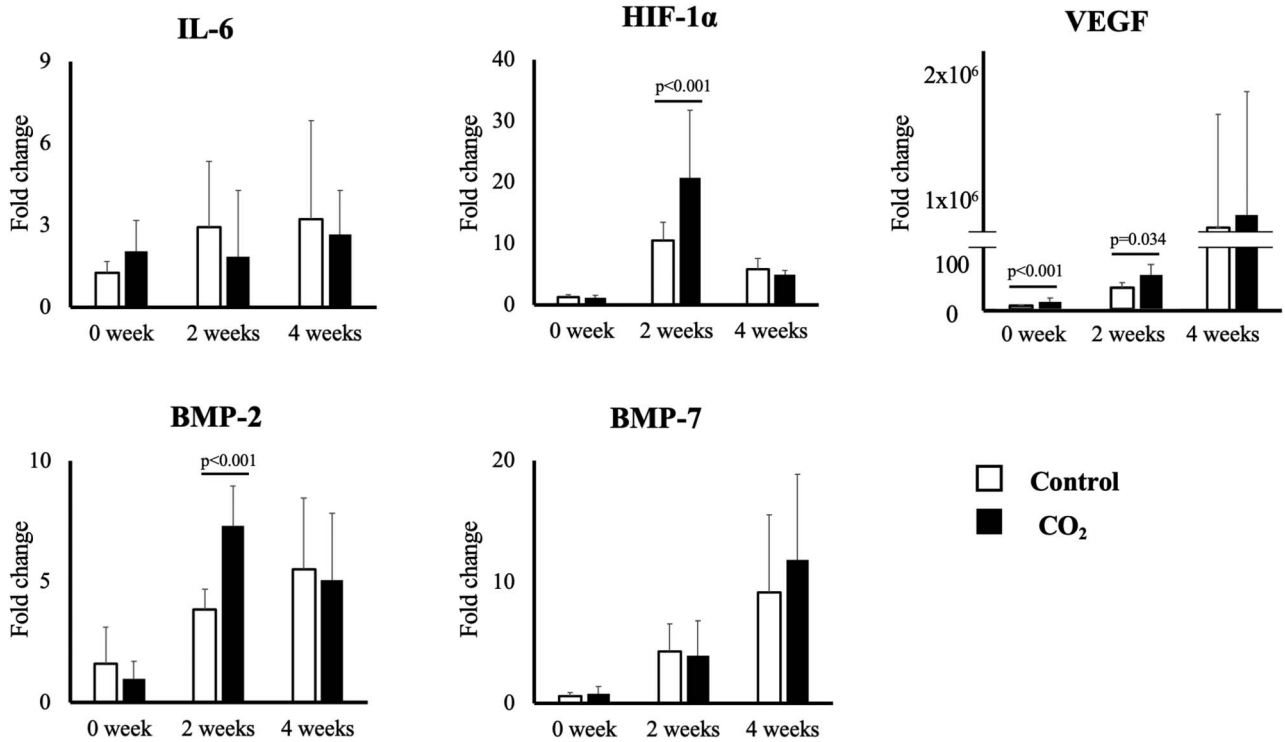


Fig. 5 This figure shows the mean (and SD) for expression of the five genes of interest in each group at each time point as measured using quantitative real-time polymerase chain reaction. The expression of HIF-1α and BMP-2 at Week 2 and the expression of VEGF at Weeks 0 and 2 were higher in the CO₂ group than in the control group.

In the histology, the cartilage at Week 2 and newly formed bone area at Week 4 were greater in the CO₂ group than the control group. This result indicated an acceleration of endochondral ossification by CO₂ therapy, which we observed in our previous study of the fracture model [30]. In some studies using distraction osteogenesis in animal models, endochondral and intramembranous ossification were observed in generated tissue. Endochondral ossification was primarily reported in studies with small animals [23, 31, 35, 41, 50], while intramembranous ossification was

observed in models of large animals such as sheep and dogs [7, 11, 13, 14, 16, 20, 21]. The difference in the modes of ossification may come from the stiffness of the fixator that was used. We used a unilateral mini-fixator, which is used in most small-animal studies. It leads to an increase in mobility in regenerated tissue, which causes the appearance of endochondral ossification foci [38]. The mode of ossification was a combination of endochondral ossification and intramembranous ossification in the current study, and relatively large cartilage tissue may have been generated. Therefore,

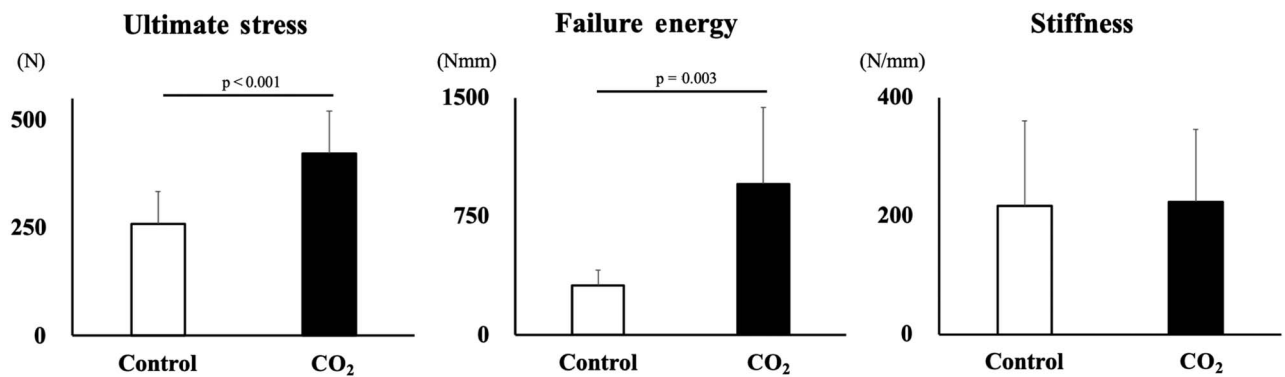


Fig. 6 This figure shows the results (mean and SD) of the three-point bend test at Week 4. Ultimate stress and failure energy were higher in the CO₂ group than in the control group.

CO₂ treatment may have accelerated bone generation effectively by enhancing endochondral ossification.

Previous studies showed that angiogenesis and blood flow are critical components of bone generation, and VEGF plays a crucial role in angiogenesis [1, 18, 26, 39]. All major VEGF ligands and interactive molecules such as neuropilin and placental growth factors have been detected in fracture sites and distraction osteogenesis sites [12, 47, 56, 57]. Evidence suggests that VEGF receptors are essential to form new blood vessels and new bone through skeletal cell differentiation [22]. In the current study, greater capillary densities were found at the distraction area at Week 0 and 2 and at the surrounding tissue area at Week 0, and the gene expression of VEGF in the distraction area was higher at Week 0 and 2 in the CO₂ group than the control group. These results indicate that CO₂ therapy might accelerate angiogenesis as well as our previous study of the fracture model [30]. BMPs are multifunctional growth factors contributing to bone formation [58], and they play important roles in regulating the major processes of fracture healing [6, 60]. Currently, two BMPs, recombinant human BMP-2 and recombinant human BMP-7, are commercially available. They have been tested in clinical trials for various bone disorders such as open fractures, nonunions, and osteonecrosis [2, 17, 55]. Additionally, recombinant human BMP-2 has been shown to accelerate bone formation in animal mandibular [5] and tibial distraction [34] models. In the current study, the gene expression of BMP-2 was higher in the CO₂ group than in the control group at Week 2 of the consolidation phase. This implies that increased blood flow and metabolism induced by CO₂ therapy might accelerate BMP-2 gene expression, and it could be why greater bone generation was observed in the CO₂ group than in the control group. A previous study revealed that the expression of HIF-1 α is upregulated under hypoxic conditions and activates the expression of angiogenic factors, thus promoting oxygen supply at the sites of skeletal generation [59]. Another study revealed that CO₂ treatment increased local oxygenation in the treated tissue [53], whereas the expression of HIF-1 α was increased at the CO₂-treated tissue in the current study. A study conducted by Mori et al. [42] using a rabbit mandibular distraction osteogenesis model also detected the strong expression of HIF-1 α in the distracted gap. These findings are discordant with previous studies. Carvalho et al. [3] reported that mechanical force was a stimulus that induced the expression of HIF-1 α mRNA, and in the current study, the mechanical force of distraction may have enhanced the expression of HIF-1 α at the distracted area. Moreover, increased blood flow because of CO₂ treatment may additionally activate the expression of HIF-1 α via enhancing metabolism. We speculate this is why the gene expression of HIF-1 α was increased in the CO₂ group in the current study.

Mechanical properties of distraction callus are factors that influence the required duration of the external fixator most directly. In the current study, the ultimate stress and failure energy at Week 4 were increased in the control group; therefore, these results support that CO₂ therapy may have a positive effect for shortening the treatment period of distraction osteogenesis.

To shorten the treatment period of distraction osteogenesis, various materials have been investigated. Kim et al. [27] examined the effect of demineralized bone matrix injection in a rabbit distraction osteogenesis model. They performed pixel value analysis for plain radiographs, as we did in our study, as well as bone mineral density analysis, micro-architecture parameter analysis and histological analysis at 0, 2, 4, and 7 days as well as at 2, 4, and 8 weeks of consolidation. The results of the pixel value analysis and the bone mineral density analysis showed higher bone density in the demineralized bone matrix group than in the control group in the third week of consolidation. Increased trabecular bone formation in the demineralized bone matrix group was observed in the third week of the consolidation period in the microarchitecture parameter analysis and the histological examination. They concluded that these results proved that the demineralized bone matrix increased the amount of regenerated bone at the distracted area. Li et al. [36] investigated the effects of bovine lactoferrin treatment on bone regeneration in distraction osteogenesis of rabbit tibia. Radiologic, histologic, bone mineral density, bone morphometric, and biomechanical analysis were performed at 4 and 8 weeks after completion of distraction in their study. The results from these analyses showed that bovine lactoferrin treatment increased bone mineral density and composition and induced better micro-CT values and biomechanical strength at 4 and 8 weeks after completion of distraction. They concluded that bovine lactoferrin treatment accelerated bone formation at an early stage and bone consolidation at a late stage of distraction osteogenesis. These studies showed positive effects of each of these materials in distraction osteogenesis of rabbit tibia, but it is difficult to compare the effectiveness between our study and their studies directly because of some differences in study designs such as time points and methods of assessment. In our previous studies in which we used a rat femoral fracture model [30] and rat femoral defect model [33], CO₂ treatment increased the gene expression of VEGF in newly generated callus tissue and the capillary density at the fracture and defect sites. Simultaneously, in the study that used a rat femoral fracture model with laser Doppler perfusion imaging, there was increased blood flow in the fractured limb [30]. Moreover, the study that used a rat femoral fracture model to assess the gene expression of collagen 2, collagen 10, and matrix metalloproteinase 13, as well as histologic assessment in both these models, indicated that endochondral ossification

was promoted [30]. Taken together, these results suggest that CO₂ treatment accelerated fracture repair and bone defect healing in association with the promotion of angiogenesis, blood flow, and endochondral ossification. In the present study, we investigated the feasibility of CO₂ treatment to accelerate bone generation in distraction osteogenesis, considering that a similar mechanism could work in these three models. The results of the current study showed increased capillary formation and VEGF expression, and early endochondral ossification along with accelerated bone generation. This implies that CO₂ treatment in the distraction osteogenesis model had similar mechanisms as in fracture repair. In this study, the change in the concentration of CO₂ in tissue during transcutaneous CO₂ treatment was not measured directly. A previous study found that transcutaneous CO₂ treatment using hydrogel decreased intramuscular pH [53]. The change in pH at the distracted site caused by CO₂ treatment may have led to the promotion of angiogenesis and blood flow. A further investigation is required to clarify whether CO₂ is absorbed into tissue at the distracted site and whether the promotion of angiogenesis, blood flow, and endochondral ossification because of CO₂ treatment is directly induced by CO₂ itself or by a secondary reaction to transcutaneous CO₂ treatment. We used unilateral fixators in this study of rabbits, whereas ring fixators or hybrid fixators are likely to be used in patients with distraction osteogenesis. Hybrid fixators are more stable and generate less cartilage tissue at the distracted site than unilateral fixators [38]. Additionally, there are differences between rabbits and humans, including body size, anatomic features, and loading mechanisms. Therefore, directly applying the study's findings clinically would not be appropriate, and further studies of larger body size animal models than rabbits such as dogs and pigs with ring or hybrid fixators are needed. The consolidation phase is the longest part of the distraction osteogenesis process, and the distraction phase also requires a long time. Although the speed of distraction may vary according to the site, many physicians usually adopt the distraction rate, or the mean distracted length per day, as 0.5 mm to 1 mm. Therefore, the distraction phase required several months when a long distraction was performed [52], and we must consider the consolidation and distraction phases. Future studies should investigate whether CO₂ treatment can increase the distraction rate. Additionally, to investigate whether or not the CO₂ therapy actually shortens the period that patients wear an external fixator, we also have to observe conditions after external fixator removal, such as fracture rate and deformity rate of the distracted limb.

In conclusion, the use of the transcutaneous application of CO₂ may open a new possibility for shortening healing time in patients with distraction osteogenesis. This method could have the potential to become attractive as a novel

additional treatment for the clinical generation and maturation of bone during distraction osteogenesis because it may be less invasive and easily accessible. However, a deeper insight into the mechanism of CO₂ in the local tissue and translational study from animal to humans are required before it can be used in future clinical practice.

Acknowledgments We thank Minako Nagata and Maya Yasuda for their kind support on histological assessment and RT-PCR assessment.

References

1. Ai-Aql ZS, Alagl AS, Graves DT, Gerstenfeld LC, Einhorn TA. Molecular mechanisms controlling bone formation during fracture healing and distraction osteogenesis. *J Dent Res*. 2008;87:107-118.
2. Calori GM, Tagliabue L, Gala L, d'Imporzano M, Peretti G, Albisetti W. Application of rhBMP-7 and platelet-rich plasma in the treatment of long bone non-unions: a prospective randomised clinical study on 120 patients. *Injury*. 2008;39:1391-1402.
3. Carvalho RS, Einhorn TA, Lehmann W, Edgar C, Al-Yamani A, Apazidis A, Pacicca D, Clemens TL, Gerstenfeld LC. The role of angiogenesis in a murine tibial model of distraction osteogenesis. *Bone*. 2004;34:849-861.
4. Chang F, Mishima H, Ishii T, Yanai T, Akaogi H, Sakai S, Yoshioka T, Ochiai N. Stimulation of EP4 receptor enhanced bone consolidation during distraction osteogenesis. *J Orthop Res*. 2007;25:221-229.
5. Cheung LK, Zheng LW. Effect of recombinant human bone morphogenetic protein-2 on mandibular distraction at different rates in an experimental model. *J Craniofac Surg*. 2006;17:100-110.
6. Cho TJ, Gerstenfeld LC, Einhorn TA. Differential temporal expression of members of the transforming growth factor beta superfamily during murine fracture healing. *J Bone Miner Res*. 2002;17:513-520.
7. Claes L, Laule J, Wenger K, Suger G, Liener U, Kinzl L. The influence of stiffness of the fixator on maturation of callus after segmental transport. *J Bone Joint Surg Br*. 2000;82:142-148.
8. Codivilla A. On the means of lengthening, in the lower limbs, the muscles and tissues which are shortened through deformity. 1904. *Clin Orthop Relat Res*. 1994:4-9.
9. Compton J, Fragomen A, Rozbruch SR. Skeletal Repair in Distraction Osteogenesis: Mechanisms and Enhancements. *JBJS Rev*. 2015;3.
10. De Bastiani G, Aldegheri R, Renzi-Brivio L, Trivella G. Limb lengthening by callus distraction (callotaxis). *J Pediatr Orthop*. 1987;7:129-134.
11. de Pablos J Jr., Canadell J. Experimental physal distraction in immature sheep. *Clin Orthop Relat Res*. 1990:73-80.
12. Deckers MM, Karperien M, van der Bent C, Yamashita T, Papapoulos SE, Lowik CW. Expression of vascular endothelial growth factors and their receptors during osteoblast differentiation. *Endocrinology*. 2000;141:1667-1674.
13. Fink B, Pollnau C, Vogel M, Skripitz R, Enderle A. Histomorphometry of distraction osteogenesis during experimental tibial lengthening. *J Orthop Trauma*. 2003;17:113-118.
14. Forriol F, Denaro L, Longo UG, Taira H, Maffulli N, Denaro V. Bone lengthening osteogenesis, a combination of intramembranous and endochondral ossification: an experimental study in sheep. *Strategies Trauma Limb Reconstr*. 2010;5:71-78.

15. Fukui T, Ii M, Shoji T, Matsumoto T, Mifune Y, Kawakami Y, Akimaru H, Kawamoto A, Kuroda T, Saito T, Tabata Y, Kuroda R, Kurosaka M, Asahara T. Therapeutic effect of local administration of low-dose simvastatin-conjugated gelatin hydrogel for fracture healing. *J Bone Miner Res*. 2012;27:1118-1131.
16. Garcia FL, Picado CH, Garcia SB. Histology of the regenerate and docking site in bone transport. *Arch Orthop Trauma Surg*. 2009;129:549-558.
17. Govender S, Csimma C, Genant HK, Valentin-Opran A, Amit Y, Arbel R, Aro H, Atar D, Bishay M, Borner MG, Chiron P, Choong P, Cinats J, Courtenay B, Feibel R, Geulette B, Gravel C, Haas N, Raschke M, Hammacher E, van der Velde D, Hardy P, Holt M, Josten C, Ketterl RL, Lindeque B, Lob G, Mathevon H, McCoy G, Marsh D, Miller R, Munting E, Oevre S, Nordsletten L, Patel A, Pohl A, Rennie W, Reynders P, Rommens PM, Rondia J, Rossouw WC, Daneel PJ, Ruff S, Ruter A, Santavirta S, Schildhauer TA, Gekle C, Schnettler R, Segal D, Seiler H, Snowdowne RB, Stapert J, Taglang G, Verdonk R, Vogels L, Weckbach A, Wentzensen A, Wisniewski T, BMPEiSfTTS Group. Recombinant human bone morphogenetic protein-2 for treatment of open tibial fractures: a prospective, controlled, randomized study of four hundred and fifty patients. *J Bone Joint Surg Am*. 2002;84:2123-2134.
18. Hankenson KD, Dishowitz M, Gray C, Schenker M. Angiogenesis in bone regeneration. *Injury*. 2011;42:556-561.
19. Hartmann BR, Bassenge E, Pittler M. Effect of carbon dioxide-enriched water and fresh water on the cutaneous microcirculation and oxygen tension in the skin of the foot. *Angiology*. 1997;48:337-343.
20. Ilizarov GA. The tension-stress effect on the genesis and growth of tissues: Part I. The influence of stability of fixation and soft-tissue preservation. *Clin Orthop Relat Res*. 1989;249-281.
21. Ilizarov GA. The tension-stress effect on the genesis and growth of tissues: Part II. The influence of the rate and frequency of distraction. *Clin Orthop Relat Res*. 1989;263-285.
22. Jacobsen KA, Al-Aql ZS, Wan C, Fitch JL, Stapleton SN, Mason ZD, Cole RM, Gilbert SR, Clemens TL, Morgan EF, Einhorn TA, Gerstenfeld LC. Bone formation during distraction osteogenesis is dependent on both VEGFR1 and VEGFR2 signaling. *J Bone Miner Res*. 2008;23:596-609.
23. Jazrawi LM, Majeska RJ, Klein ML, Kagel E, Stromberg L, Einhorn TA. Bone and cartilage formation in an experimental model of distraction osteogenesis. *J Orthop Trauma*. 1998;12:111-116.
24. Jensen FB. Red blood cell pH, the Bohr effect, and other oxygenation-linked phenomena in blood O₂ and CO₂ transport. *Acta Physiol Scand*. 2004;182:215-227.
25. Kawamoto T, Kawamoto K. Preparation of thin frozen sections from nonfixed and undecalcified hard tissues using Kawamoto's film method (2012). *Methods Mol Biol*. 2014;1130:149-164.
26. Keramaris NC, Calori GM, Nikolaou VS, Schemitsch EH, Giannoudis PV. Fracture vascularity and bone healing: a systematic review of the role of VEGF. *Injury*. 2008;39 Suppl 2: S45-57.
27. Kim JB, Lee DY, Seo SG, Kim EJ, Kim JH, Yoo WJ, Cho TJ, Choi IH. Demineralized Bone Matrix Injection in Consolidation Phase Enhances Bone Regeneration in Distraction Osteogenesis via Endochondral Bone Formation. *Clin Orthop Surg*. 2015;7:383-391.
28. Kitoh H, Kitakoji T, Tsuchiya H, Katoh M, Ishiguro N. Transplantation of culture expanded bone marrow cells and platelet rich plasma in distraction osteogenesis of the long bones. *Bone*. 2007;40:522-528.
29. Kitoh H, Kitakoji T, Tsuchiya H, Mitsuyama H, Nakamura H, Katoh M, Ishiguro N. Transplantation of marrow-derived mesenchymal stem cells and platelet-rich plasma during distraction osteogenesis—a preliminary result of three cases. *Bone*. 2004;35:892-898.
30. Koga T, Niikura T, Lee SY, Okumachi E, Ueha T, Iwakura T, Sakai Y, Miwa M, Kuroda R, Kurosaka M. Topical cutaneous CO₂ application by means of a novel hydrogel accelerates fracture repair in rats. *J Bone Joint Surg Am*. 2014;96:2077-2084.
31. Kojimoto H, Yasui N, Goto T, Matsuda S, Shimomura Y. Bone lengthening in rabbits by callus distraction. The role of periosteum and endosteum. *J Bone Joint Surg Br*. 1988;70:543-549.
32. Korzinek K, Tepic S, Perren SM. Limb lengthening and three-dimensional deformity corrections. A retrospective clinical study. *Arch Orthop Trauma Surg*. 1990;109:334-340.
33. Kuroiwa Y, Fukui T, Takahara S, Lee SY, Oe K, Arakura M, Kumabe Y, Oda T, Matsumoto T, Matsushita T, Akisue T, Sakai Y, Kuroda R, Niikura T. Topical cutaneous application of CO₂ accelerates bone healing in a rat femoral defect model. *BMC Musculoskelet Disord*. 2019;20:237.
34. Li G, Boussein ML, Luppen C, Li XJ, Wood M, Seeherman HJ, Wozney JM, Simpson H. Bone consolidation is enhanced by rhBMP-2 in a rabbit model of distraction osteogenesis. *J Orthop Res*. 2002;20:779-788.
35. Li G, Simpson AH, Kenwright J, Triffitt JT. Effect of lengthening rate on angiogenesis during distraction osteogenesis. *J Orthop Res*. 1999;17:362-367.
36. Li W, Zhu S, Hu J. Bone Regeneration Is Promoted by Orally Administered Bovine Lactoferrin in a Rabbit Tibial Distraction Osteogenesis Model. *Clin Orthop Relat Res*. 2015;473 {Nicholas, 2015 #271}:2383-2393.
37. Livak KJ, Schmittgen TD. Analysis of relative gene expression data using real-time quantitative PCR and the 2(-Delta C(T)) Method. *Methods*. 2001;25:402-408.
38. Lopez-Pliego EM, Giraldez-Sanchez MA, Mora-Macias J, Reina-Romo E, Dominguez J. Histological evolution of the regenerate during bone transport: an experimental study in sheep. *Injury*. 2016;47 Suppl 3:S7-S14.
39. Marsell R, Einhorn TA. The biology of fracture healing. *Injury*. 2011;42:551-555.
40. Maruno H. Effects of intermittent administration of parathyroid hormone on distraction osteogenesis in rabbits. *J Kyorin Med Soc*. 2011;42:29-38.
41. Mizuta H, Nakamura E, Mizumoto Y, Kudo S, Takagi K. Effect of distraction frequency on bone formation during bone lengthening: a study in chickens. *Acta Orthop Scand*. 2003;74:709-713.
42. Mori S, Akagi M, Kikuyama A, Yasuda Y, Hamanishi C. Axial shortening during distraction osteogenesis leads to enhanced bone formation in a rabbit model through the HIF-1alpha/vascular endothelial growth factor system. *J Orthop Res*. 2006;24:653-663.
43. Moseley CF. Assessment and prediction in leg-length discrepancy. *Instr Course Lect*. 1989;38:325-330.
44. Moseley CF. Leg lengthening. A review of 30 years. *Clin Orthop Relat Res*. 1989;38-43.
45. Oe K, Ueha T, Sakai Y, Niikura T, Lee SY, Koh A, Hasegawa T, Tanaka M, Miwa M, Kurosaka M. The effect of transcutaneous application of carbon dioxide (CO₂) on skeletal muscle. *Biochem Biophys Res Commun*. 2011;407:148-152.
46. Okazaki H, Kurokawa T, Nakamura K, Matsushita T, Mamada K, Kawaguchi H. Stimulation of bone formation by recombinant fibroblast growth factor-2 in callotaxis bone lengthening of rabbits. *Calcif Tissue Int*. 1999;64:542-546.

47. Pacicca DM, Patel N, Lee C, Salisbury K, Lehmann W, Carvalho R, Gerstenfeld LC, Einhorn TA. Expression of angiogenic factors during distraction osteogenesis. *Bone*. 2003;33:889-898.
48. Paley D. Problems, obstacles, and complications of limb lengthening by the Ilizarov technique. *Clin Orthop Relat Res*. 1990;81-104.
49. Resch KL, Just U. [Possibilities and limits of CO₂ balneotherapy]. [in German]. *Wiener medizinische Wochenschrift* (1946). 1994;144:45-50.
50. Richards M, Goulet JA, Schaffler MB, Goldstein SA. Temporal and spatial characterization of regenerate bone in the lengthened rabbit tibia. *J Bone Miner Res*. 1999;14:1978-1986.
51. Saghie S, Khoury NJ, Tawil A, Masrouha KZ, Musallam KM, Khalaf K, Dosh L, Jaouhari RR, Birjawi G, El-Hajj-Fuleihan G. The impact of zoledronic acid on regenerate and native bone after consolidation and removal of the external fixator: an animal model study. *Bone*. 2010;46:363-368.
52. Sailhan F. Bone lengthening (distraction osteogenesis): a literature review. *Osteoporos Int*. 2011;22:2011-2015.
53. Sakai Y, Miwa M, Oe K, Ueha T, Koh A, Niikura T, Iwakura T, Lee SY, Tanaka M, Kurosaka M. A novel system for transcutaneous application of carbon dioxide causing an "artificial Bohr effect" in the human body. *PLoS One*. 2011;6:e24137.
54. Song H-R, Oh C-W, Kyung H-S, Park I-H, Kim P-T, Baek S-H, Kim S-J, Lee S-T. Injected calcium sulfate for consolidation of distraction osteogenesis in rabbit tibia. *J Pediatr Orthop B*. 2004;13:170-175.
55. Sun W, Li Z, Gao F, Shi Z, Zhang Q, Guo W. Recombinant human bone morphogenetic protein-2 in debridement and impacted bone graft for the treatment of femoral head osteonecrosis. *PLoS One*. 2014;9:e100424.
56. Tombran-Tink J, Barnstable CJ. Osteoblasts and osteoclasts express PEDF, VEGF-A isoforms, and VEGF receptors: possible mediators of angiogenesis and matrix remodeling in the bone. *Biochem Biophys Res Commun*. 2004;316:573-579.
57. Uchida S, Sakai A, Kudo H, Otomo H, Watanuki M, Tanaka M, Nagashima M, Nakamura T. Vascular endothelial growth factor is expressed along with its receptors during the healing process of bone and bone marrow after drill-hole injury in rats. *Bone*. 2003;32:491-501.
58. Urist MR. Bone: formation by autoinduction. *Science*. 1965;150:893-899.
59. Wang Y, Wan C, Deng L, Liu X, Cao X, Gilbert SR, Bouxsein ML, Faugere MC, Guldberg RE, Gerstenfeld LC, Haase VH, Johnson RS, Schipani E, Clemens TL. The hypoxia-inducible factor alpha pathway couples angiogenesis to osteogenesis during skeletal development. *J Clin Invest*. 2007;117:1616-1626.
60. Yu YY, Lieu S, Lu C, Miclau T, Marcucio RS, Colnot C. Immunolocalization of BMPs, BMP antagonists, receptors, and effectors during fracture repair. *Bone*. 2010;46:841-851.
61. Zakhary K, Motakis D, Hamdy RH, Campisi P, Amar Y, Lessard ML. Effect of recombinant human bone morphogenetic protein 7 on bone density during distraction osteogenesis of the rabbit mandible. *J Otolaryngol*. 2005;34:407-414.
62. Zheng LW, Cheung LK. Effect of recombinant human bone morphogenetic protein-2 on mandibular distraction at different rates in a rabbit model. *Tissue Eng*. 2006;12:3181-3188.